

Quantum phase space with a basis of Wannier functions

Yuan Fang,¹ Fan Wu,¹ and Biao Wu^{1,2,3,*}

¹*International Center for Quantum Materials, School of Physics, Peking University, Beijing 100871, China*

²*Collaborative Innovation Center of Quantum Matter, Beijing 100871, China*

³*Wilczek Quantum Center, School of Physics and Astronomy,
Shanghai Jiao Tong University, Shanghai 200240, China*

(Dated: March 12, 2022)

A quantum phase space with Wannier basis is constructed: (i) classical phase space is divided into Planck cells; (ii) a complete set of Wannier functions are constructed with the combination of Kohn's method and Löwdin method such that each Wannier function is localized at a Planck cell. With these Wannier functions one can map a wave function unitarily onto phase space. Various examples are used to illustrate our method and compare it to Wigner function. The advantage of our method is that it can smooth out the oscillations in wave functions without losing any information and is potentially a better tool in studying quantum-classical correspondence. In addition, we point out that our method can be used for time-frequency analysis of signals.

I. INTRODUCTION

Phase space, where every point represents a state in a classical dynamical system, is not only a fundamental concept but also an important tool in classical mechanics. In contrast, in quantum mechanics, the fact that position and momentum operators are not commutative results in the difficulty of proper definition of quantum phase space. Nevertheless, physicists have tried various ways to adapt phase space into quantum mechanics. One famous example is the reformulation of quantum mechanics in phase space with path integral by Feynman [1].

Another well-known example is Wigner function, which gives a representation of wave function in phase space [2]. Later Husimi developed Q representation while Sudarshan and Glauber developed P representation in phase space for wave function [3–5]. However, all these three methods can only give us *quasi*-probability distributions in phase space: The Wigner function and Sudarshan-Glauber P function can be negative; for the Husimi Q function, its marginal distribution for a pure state ψ does not equal to $|\psi|^2$. Despite these drawbacks, we have seen tremendous developments of all these methods over the years because they are natural bridges between quantum and classical dynamics and also have many practical applications in quantum optics, nuclear and particle physics, condensed matter and mesoscopic systems [6, 7].

In 1929 von Neumann already suggested a different way to map a wave function onto phase space [8, 9]. In von Neumann's method, one divides classical phase space into Planck cells and then finds a set of orthonormal wave functions which are localized at these Planck cells. With these orthonormal wave functions served as a basis, a wave function is mapped unitarily to phase space, and the amplitudes at the Planck cells give us a true probability

distribution. Von Neumann's motivation was to establish quantum phase space so that he could borrow many ideas from classical statistical physics to set up a foundational framework for quantum statistical physics [8, 9].

However, von Neumann only showed how these localized wave functions could be found in principle but did not offer an efficient approach to compute them. Von Neumann's method was developed in a recent work [10] where Kohn's orthogonalization method [11] was employed and a set of Wannier functions localized at Planck cells were found.

In this work we further develop this quantum phase space with Wannier functions as its basis. We find a more efficient approach to compute these Wannier functions by using Löwdin's orthogonalization method [12, 13] on top of the Kohn's method [11]. With this Wannier basis, a wave function can be mapped unitarily onto phase space. The amplitude at each Planck cell is complex in general and, however, due to the unitarity of this mapping, the square of its amplitude magnitude is *true* probability. This is the crucial difference between our method and well-known Wigner, P or Q function. The latter can only give us quasi-probability. With our method, it is now possible to test numerically many fundamental ideas proposed by von Neumann in 1929 [8, 9].

Using various concrete examples, we compare our unitary mapping to Wigner function. There are two key features in the comparison. (i) Our unitary mapping is very effective to smooth out the oscillations in a wave function and produces a probability distribution that in some cases resembles a classical trajectory while the Wigner function can not. (ii) The Wigner function is coarse-grained by averaging over Planck cells; the resulting distribution is very different from the original Wigner function but very similar to the true probability distribution obtained with our method. This shows that one can roughly get a probability distribution in phase space by coarse-graining Wigner function. However, a lot of information is lost to with coarse-graining whereas our unitary mapping does not lose any information. Such a comparison shows that our unitary mapping can be an

*Electronic address: wubiao@pku.edu.cn

excellent tool for studying the quantum-classical correspondence, the central theme of quantum chaos [14]. In the end, we further point out that our method can be used for time-frequency signal analysis.

The rest of this paper is organized as follows. In Section II, von Neumann's method is reviewed along with the work in Ref. [10]. In Section III, our method is described in detail. We then discuss how localized our Wannier functions are in Section IV. In Section V, we compare our unitary projection to Wigner function with various examples. In Section VI, we use an example to show how our method can be applied to signal analysis. In the end we draw some conclusions in Section VII.

II. REVIEW OF VON NEUMANN'S METHOD

Von Neumann in 1929 suggested a method to construct quantum phase space [8, 9], which consists with two steps: (i) dividing the classical phase space into Planck cells; (ii) finding a set of orthonormal wave functions which are localized at Planck cells. Von Neumann suggested to find these orthonormal wave functions by orthogonalizing a set of Gaussian wave packets of width ζ with the Schmidt method,

$$g_{j_x, j_k} \equiv \exp \left[-\frac{(x - j_x x_0)^2}{4\zeta^2} + i j_k k_0 x \right] \quad (1)$$

where j_x and j_k are integers. When $x_0 k_0 = 2\pi$, this set of Gaussian packets is complete.

This method shows that in principle one can map a wave function unitarily onto phase space and establish a probability distribution for a quantum state in phase space. This proof of principle was enough for von Neumann to prove in an abstract way of quantum ergodic theorem and quantum H theorem [8, 9].

However, von Neumann's construction is not very computationally practical due to the following drawbacks:

- i) The Schmidt orthogonalization procedure is computationally costly, rendering it numerically not feasible.
- ii) The wave functions constructed in this way lack spatial translational symmetry. Since there should be no difference of measuring coordinates at different sites, such a symmetry is desired.
- iii) This method is very sensitive to the order of the orthogonalization procedure and will produce base functions with large tails (or standard deviations) bearing little resemblance to the original Gaussian functions.

In Ref. [10], Han and Wu were able to remove the second drawback. In their approach, the subscript j_k is treated as band index and the Gaussian wave packets with the same j_k are orthonormalized with Kohn's approach [11] to become a set of Wannier functions whose

spacial translational symmetry is guaranteed. At the same time, the computational cost is reduced substantially such that the whole method is now computationally feasible. However, the orthogonalization among Gaussian wave functions with different j_k is still Schmidt and the third drawback remains. In this work we employ Löwdin orthogonalization method [12] on top of Kohn's method. As the Löwdin orthogonalization produces a set of orthonormal vectors which are the most faithful to the original non-orthogonal vectors [13], the orthogonalization result is unique and independent of order of orthogonalization. So the third drawback is removed. Furthermore, the Löwdin method is more efficient and can reduce the computational cost dramatically.

In Ref. [8, 9], von Neumann proposed many fundamental ideas using his quantum phase space; however, these ideas had remained on the abstract level before our work. For example, von Neumann defined an entropy for pure quantum states using the probability distribution in his quantum phase space. However, there was no practical way to compute this entropy. With our method, we can now compute such an entropy numerically [10].

III. OUR METHOD

We focus on two dimensional phase spaces. Generalization to higher dimensions are straightforward as done in Ref.[10]. The detailed procedure of our method is elaborated as follows.

- i) Choose an initial set of localized wave packets such as the Gaussian wave packets $g_{j_k}(x) \equiv g_{0, j_k}(x)$ in Eq.(1). Find their Fourier transform $\tilde{g}_{j_k}(k) \equiv \mathcal{F}\{g_{j_k}(x)\}$. In our calculations, we choose $x_0 = 1, k_0 = 2\pi, \zeta = (2\pi)^{-1}$, and we have

$$\tilde{g}_{j_k}(k) \equiv \exp \left[-\left(\frac{k}{2\pi} - j_k\right)^2 \right]. \quad (2)$$

- ii) At a fixed $k \in [0, 2\pi)$, for each j_k , we construct a columnwise vector whose n th element is $\tilde{g}_{j_k}(k + 2n\pi)$. We denote this vector by f_{k, j_k} .

$$f_{k, j_k} = [\tilde{g}_{j_k}(k + 2n\pi)]_{n \in \mathbb{Z}}^T, \quad (3)$$

where the superscript T represents transpose. In numerical calculation, one needs to choose a cut-off N so that $-N \leq n \leq N$. These vectors f_{k, j_k} with different j_k are not orthogonal to each other.

- iii) Apply Löwdin orthogonalization to f_{k, j_k} : (a) put these vectors together to form a matrix

$$F \equiv [f_{k, -J_k}, \dots, f_{k, j_k}, f_{k, (j_k+1)}, \dots, f_{k, J_k}] \quad (4)$$

where J_k is the cut-off for j_k ; (b) the matrix of the orthonormalized vectors is

$$\begin{aligned} & [u_{k, -J_k}, \dots, u_{k, j_k}, u_{k, (j_k+1)}, \dots, u_{k, J_k}] \\ & = F(F^\dagger F)^{-\frac{1}{2}}; \end{aligned} \quad (5)$$

(c) let $\tilde{w}_{j_k}(k + 2n\pi) = u_{k,j_k}(n)/\sqrt{2\pi}$.

iv) The interval $[0, 2\pi)$ is evenly divided into N_k points in numerical calculations. For every k of these N_k points, repeat step (ii) and step (iii). Finally, after Fourier transform, we get a set of orthonormal basis of Wannier functions $\{w_{j_x, j_k}\}$,

$$w_{j_x, j_k}(x) \equiv w_{j_k}(x - j_x). \quad (6)$$

For simplicity, from now on we will adopt Dirac notation and let $|w_j\rangle = |w_{j_x, j_k}\rangle$, where (j_x, j_k) is simplified to j whenever no confusion arises. Note that in our calculation we set $N_k = 2J_k$.

For these wave functions $|w_j\rangle$, the relation $\langle w_{j_x, j_k} | w_{j'_x, j'_k} \rangle = \delta_{j_k, j'_k}$ is guaranteed explicitly by the Löwdin orthogonalization in the above procedure and the relation $\langle w_{j_x, j_k} | w_{j'_x, j'_k} \rangle = \delta_{j_x, j'_x}$ is guaranteed implicitly by Kohn's method. The full orthonormal relation $\langle w_j | w_{j'} \rangle = \delta_{j, j'}$ is then achieved. Note that for a given set of non-orthogonal vector the Löwdin orthogonalization produces a unique set of orthonormal vectors [12, 13]. In contrast, the result of the Schmidt orthogonalization depends on the order of orthogonalization. As a result, our procedure gives rise to a unique set of Wannier functions once the initial trial wave function, such as the Gaussians in Eq.(1), are given. This removes the third drawback in von Neumann's method. At the same time, it reduces further the computational cost.

As pointed out above, although they are not orthonormal, the Gaussian wave functions in Eq.(1) are a complete set of basis when $x_0 k_0 = 2\pi$. This is already implicitly mentioned by von Neumann [8, 9]. Consequently, the Wannier functions constructed out of these Gaussian functions with our method form a complete set of orthonormal basis. This means that the volume of a Planck cell is $x_0 p_0 = x_0 \hbar k_0 = 2\pi \hbar = h$ with h being the Planck constant.

We summarize the basic feature of our quantum phase space: (1) It is made of Planck cells; (2) each Planck cell is assigned a Wannier function $|w_j\rangle$; (3) all the Wannier functions form a complete set of orthonormal basis. Any given wave function $|\psi\rangle$ can now be mapped onto our quantum phase space

$$|\psi\rangle = \sum_j |w_j\rangle \langle w_j | \psi \rangle. \quad (7)$$

We emphasize that this mapping is linear and unitary, which is different from Wigner function, P representation, or Q representation that are nonlinear and not unitary. As a result, $p_j = |\langle w_j | \psi \rangle|^2$ is the probability at Planck cell j , a true probability distribution over phase space.

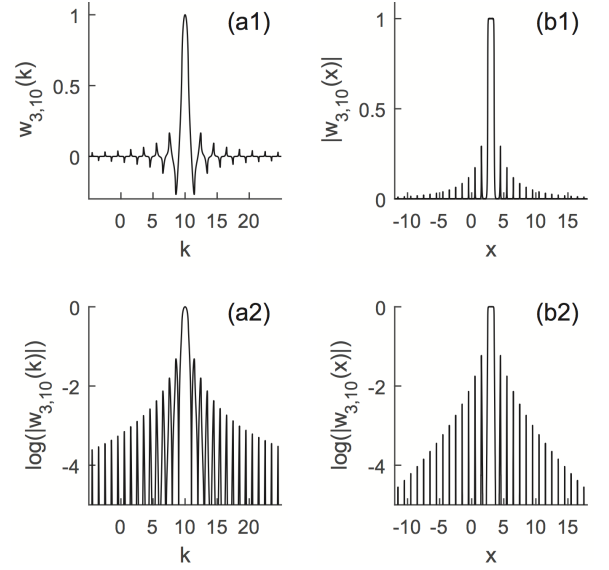


FIG. 1: (a1,a2) Wannier function $w_{3,10}$ in the k space; (b1,b2) Wannier function $w_{3,10}$ in the x space. In k space, the Wannier function is real and plotted directly; in x space, the Wannier function is complex and its amplitude is plotted. In the lower two panels, the amplitude of $w_{3,10}$ is plotted in the semi-log format, showing exponentially decaying tails in both x and k spaces. The unit of x is x_0 and the unit of k is k_0 . In our calculation, $J_k = 40$, $N_k = 80$, and $N = 50$.

IV. LOCALIZATION OF WANNIER FUNCTIONS

In this section we examine how localized the above Wannier functions are. Shown in Fig.1 is one typical Wannier function $w_{3,10}$ in both k space and x space. This Wannier function is localized near the site ($x = 3$, $k = 10 \times 2\pi$) and is obtained by choosing $J_k = 40$, $N_k = 80$, and $N = 50$ with our method. It is clear from the two lower panels which are the semi-log plots of their counterparts in the upper panels that the Wannier function is exponentially localized in both k space and x space.

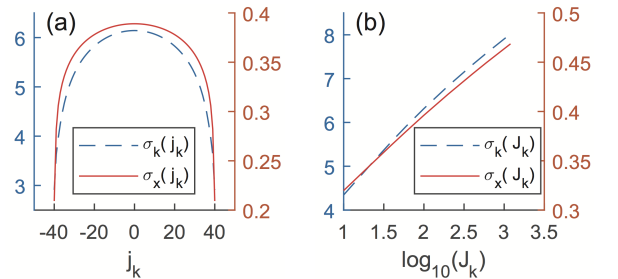


FIG. 2: (color online) (a) The widths σ_x (red) and σ_k (blue) of Wannier functions in both x and k spaces as functions of j_k . $J_k = 40$, $N_k = 80$, and $N = 50$. (b) The widths σ_x and σ_k at $j_k = 0$ as function of J_k , the cut-off of j_k . $N_k = 2J_k$ and $N = 50$.

To measure the localization quantitatively, we use the standard deviation that is defined as

$$\sigma_x(j) = \langle w_j | (x - \langle x \rangle_j)^2 | w_j \rangle^{\frac{1}{2}} \quad (8)$$

$$\sigma_k(j) = \langle w_j | (k - \langle k \rangle_j)^2 | w_j \rangle^{\frac{1}{2}} \quad (9)$$

As Wannier functions have translational symmetry with respect to j_x , which is ensured by Khon's method, we only need to consider Wannier functions w_{0,j_k} . Fig.2(a) illustrates how the standard deviations of these Wannier functions change with j_k . The figure shows that both σ_x and σ_k have maximal values at $j_k = 0$ and then decrease monotonically when $|j_k|$ increases. At the two ends where $|j_k|$ is large, we roughly have $\sigma_x \cdot \sigma_k \sim 0.5$, the lower limit of any wave packet demanded by the uncertainty relation. Both σ_x and σ_k are much larger, consequently, $\sigma_x \cdot \sigma_k$ is much larger than 0.5 when $|j_k|$ is small.

When the size of quantum phase space in our numerical calculation, i.e., the cut-off J_k increases, we find that the maximal values of both σ_x and σ_k increase. These two monotonic relations are plotted in Fig.2(b). The data in the figure apparently show that the increase of both $\sigma_x(j_k = 0)$ and $\sigma_k(j_k = 0)$ with J_k is sub-logrithmic. This suggests that both σ_x and σ_k may have finite upper limits. Bourgain proved that such a basis exists in principle [15]. However, Bourgain's approach of construction also involves Schmidt orthogonalization, which is computationally expensive.

V. COMPARISON WITH WIGNER FUNCTION

Our construction of quantum phase space yields a natural way to map a wave function onto phase space as in Eq.(7). Here we compare it to existing methods that map a wave function onto phase space. We focus on Wigner function as it is the most widely used method [6]. The differences between Wigner function and our method are obvious: (i) Wigner function is a nonlinear mapping while ours is a linear unitary mapping; (ii) Wigner function is real and continuous in phase space while ours produces a discrete and complex function in phase space. However, as we will see, they bear some similarity after Wigner function is coarse-grained.

Wigner function (or Weyl transform of density matrix) of a wave function $\psi(x)$ is defined as [2, 6]

$$W(x, k) = \frac{1}{\pi} \int \psi^*(x+y) \psi(x-y) e^{2iky} dy. \quad (10)$$

The Wigner function can be coarse-grained with a function $h(x, k)$ that is localized in phase space

$$W_h(x, k) = \int h(x' - x, k' - k) W(x', k') dx' dk'. \quad (11)$$

The function $h(x, k)$ is usually chosen to be localized at a Planck cell. One popular choice is $h(x, k) =$

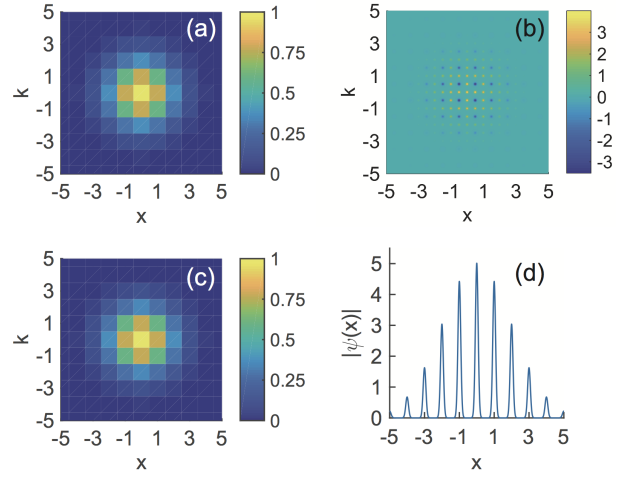


FIG. 3: (color online) (a) Gaussian packet in our quantum phase space with the Wannier basis; (b) the corresponding Wigner function, where the negative parts are surrounded by positive parts; (c) the discrete coarse-grained Wigner function; (d) the amplitude in the x space. The unit of x is x_0 and the unit of k is k_0 .

$\frac{1}{\pi} \exp(-\frac{x^2}{\sigma_x^2} - \frac{k^2}{\sigma_k^2})$ with $\sigma_x \sigma_k = \frac{1}{2}$ [6]. In our calculation, we choose

$$h(x, k) = \left[H\left(x + \frac{1}{2}\right) - H\left(x - \frac{1}{2}\right) \right] \times \left[H\left(k + \frac{1}{2}\right) - H\left(k - \frac{1}{2}\right) \right], \quad (12)$$

where $H(x)$ is the Heaviside function. This h function is intuitively simple as it facilitates an integration precisely over a Planck cell. We shall use some typical and simple examples to compare our unitary projection to Wigner function.

A. Gaussian packet in our quantum phase space

As the first example, we consider the following wave function

$$\psi(x) = \sum_{j_x, j_k} w_{j_x, j_k}(x) e^{-j_x^2 - j_k^2}. \quad (13)$$

This wave function can be regarded as a discrete Gaussian packet in our quantum phase space as shown in Fig.3(a). It is positive in every Planck cell. In contrast, as seen in Fig.3(b), its corresponding Wigner function has either positive or negative values. Interestingly, this Wigner function becomes significantly different from zero only at integer or half integer coordinates. Its negative spots at half integer coordinates are surrounded by positive spots at integer coordinates. This is a reflection of the oscillations of the wave function $\psi(x)$ in the x space (see Fig.3(d)).

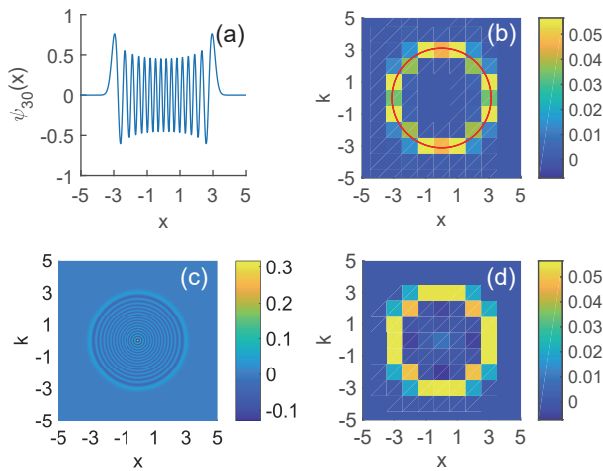


FIG. 4: (color online) The 30th energy eigenstate of an harmonic oscillator. (a) Its wave function in the x space; (b) its unitary projection onto our quantum phase space (the red circle is the corresponding classical trajectory); (c) its Wigner function; (d) its discrete coarse-grained Wigner function. The unit of x is x_0 and the unit of k is k_0 .

The coarse-grained Wigner function is plotted in Fig.3(c). Its overall feature looks very similar to Fig.3(a). Despite this similarity, we need to bear in mind that this coarse-grained Wigner function does not give probability at a given Planck cell. Later we will show an example, where the coarse-grained Wigner function can still be negative at some Planck cells. By coarse-graining, some information is lost while the projection with our Wannier basis is unitary and no information is lost.

As any smooth function can be roughly regarded as a superposition of many Gaussian functions, what we observe from this typical example is quite general: (i) Our unitary projection onto the quantum phase space is very effective in smoothing out the oscillations in wave function while Wigner function is not. (ii) Wigner function gives us only quasi-probability; it is still a quasi-probability when averaged over a finite region such as a Planck cell. However, from the similarity between the coarse-grained Wigner function and our unitary projection (Fig. 3(b) vs. (c)), one can conclude that the quasi-probability distribution of a coarse-grained Wigner function can be roughly regarded as a true probability distribution. In a sense, one can not claim this with great confidence before our work: there was no unitary mapping to phase space before our work and therefore no true probability distribution; without comparison to a true probability distribution, one would not know how close a coarse-grained Wigner function is to a true probability distribution. As our method can give rise to a true probability distribution, one is then allowed to use it to define an entropy for pure quantum states [8–10] One can not use Wigner function with or without coarse-graining for this purpose.

B. Harmonic Oscillator

Harmonic Oscillator is one of the simplest problems in quantum mechanics. Its n th energy eigenfunction is

$$\psi_n(x) = \left(\frac{1}{2^n n!}\right)^{1/2} \pi^{-1/4} \exp(-x^2/2) H_n(x), \quad (14)$$

where $H_n(x)$ are the Hermite polynomials. We choose $n = 30$. The wave function of ψ_{30} in the x space is shown in Fig.4(a). And its unitary projection onto our quantum phase space is shown in Fig.4(b) where we see that the wave function has significant weights along the classical orbit. As in the first example, the oscillations in $\psi_{30}(x)$ have disappeared in the Wannier representation. Looking more carefully, one can find that the weights near grids (3,0) and (0,3) are a slightly different. It is because our Wannier basis does not have translational symmetry in the k direction.

One very important feature in Fig.4(b) is that most of the probabilities concentrate along a circle, which is the corresponding classical trajectory. This is not the case for the corresponding Wigner function. The Wigner function is shown on Fig.4(c) where we can see 15 circles, a reflection of the oscillations in $\psi_{30}(x)$. The center has the largest density of distribution. Therefore, our unitary projection can produce a probability distribution that resembles a classical trajectory while Wigner function can not. In fact, we have applied our method to more sophisticated systems, where the quantum probability distribution in phase space obtained with our method bears strikingly similarity to its classical ensemble distribution in phase space. Unfortunately, these results are beyond this work and will be presented elsewhere. This shows that our unitary projection is a better tool to establish quantum-classical correspondence, the central subject in quantum chaos [14].

Fig.4(d) illustrates the coarse-grained Wigner function whose overall features look quite similar to Fig.4(b). However, there are minor differences, for example, it is symmetric in both x and k directions and it is positive at the center (0,0). We note one important feature: the coarse-grained Wigner function is negative at $(\pm 2, 0)$ and $(0, \pm 2)$. This shows that the coarse graining with the chosen h function in Eq. (12) does not guarantee positive value at a given Planck cell. Despite its similarity to our unitary projection, a coarse-grained Wigner function is still a quasi-probability.

C. Schödinger cat state

In quantum optics, a cat state is defined as the superposition of two coherent states with opposite phase:

$$|\text{cat}\rangle = |\alpha\rangle + |-\alpha\rangle = 2e^{\frac{-|\alpha|^2}{2}} \sum_n \frac{\alpha^{2n}}{\sqrt{(2n)!}} |2n\rangle, \quad (15)$$

where $|2n\rangle$ is a Fock state with $2n$ particles. In our calculation, we choose $\alpha = 3 + 3i$. The wave function in the x

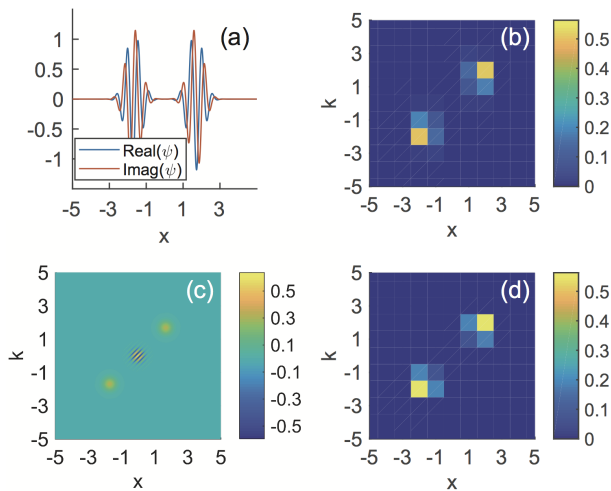


FIG. 5: (color online) Schrodinger cat state $|\text{cat}\rangle = |\alpha\rangle + |-\alpha\rangle$ with $\alpha = 3 + 3i$. (a) Its wave function in the x space; (b) its unitary projection onto the quantum phase space; (c) its Wigner function; (d) its discrete coarse-grained Wigner function. The unit of x is x_0 and the unit of k is k_0 .

space is shown on Fig.5(a). The wave function looks like two moving Gaussian packets localized near $x = -2$ and $x = 2$. Its unitary projection onto the quantum phase space is shown on Fig.5(b). The wave function looks again rather smooth in the quantum phase space and is localized around two regions.

Its Wigner function is plotted in Fig.5 (c) and it has a rapidly oscillating center, which is regarded as an iconic feature of a coherent cat state [16]. However, this oscillating center disappears in the coarse-grained Wigner function in Fig.5(d) and in our unitary projection in Fig.5(b). This means that the probability around this center is in fact close to zero.

With the examples above, we can conclude that our unitary projection of a wave function onto quantum phase space with the Wannier basis produces a result looking very similar to the coarse-grained Wigner function. This has two implications: (i) Our unitary project is very effective to smooth out the oscillations in a wave function. However, our projection is unitary and does not lose any information while a lot of information is lost in the coarse-graining. (ii) As a result, our unitary project can produce a true probability distribution resembling a classical trajectory as most dramatically seen with the example of harmonic oscillator. The oscillations between positive and negative values in Wigner functions (see Figs.3(b), 4(c)&5(c)) are regarded as an indication of “quantumness” in the quantum state [6, 16]. However, this also makes it difficult to build a connection between quantum dynamics and classical dynamics in phase space. One way to go around this difficulty is to remove some information of a wave function, i.e., coarse-graining. Our unitary projection can achieve this goal without losing any information. The reason is that the oscillations are hidden in the Wannier basis. Therefore, our uni-

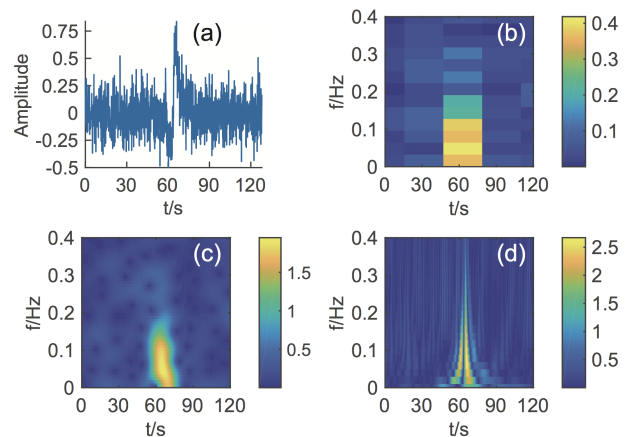


FIG. 6: (color online) (a) A signal with noise; (b) time-frequency analysis with our Wannier basis; (c) time-frequency analysis with the short-time Fourier transform; (d) time-frequency analysis with a wavelet method.

tary projection is a better tool in studying the quantum-classical correspondence in phase space. It will also be interesting to compare our method to Wigner function in other applications such as in quantum optics [7]. This is beyond the scope of this work.

VI. APPLICATION IN TIME-FREQUENCY SIGNAL ANALYSIS

Similar to Wigner function, our method can be applied to any pair of variables which are related to each other by Fourier transform; therefore, our method has a potential in application of time-frequency signal analysis which is used to characterize and manipulate signals whose statistics vary in time, such as transient signals.

In the past decades, many time-frequency analysing techniques have been devised [17]. Wavelets and short-time Fourier transform are two most prevalent methods. We compare our method with these techniques for a simulated example. The most important goal in signal analysis is to extract the signal from the noise. So a testing signal is designed with a random noise and it is shown in Fig.6 (a). Fig.6 (b), (c), and (d) are results of our method, short-time Fourier transform, and wavelet, respectively. Our method works as well as the other two methods to identify the signal. However, it is clear from Fig.6 (b) that the result produced with our method is much more compact when stored on computer. In addition, our method with Wannier basis has the same frequency resolution for the whole frequency spectrum; in contrast, wavelet has lower frequency resolution for high frequencies. This means that our method should be better than wavelet when dealing with problems that require high frequency-resolution in regions with high frequencies.

VII. CONCLUSIONS

We have developed a method that can map a wave function unitarily onto phase space with a complete set of localized Wannier functions. Our method is significantly improved over the von-Nuemann's method and a method in Ref.[10] with the use of the Löwdin's orthogonalization. This approach is not only independent of orthogonalization order but also more numerically efficient. Various examples are used to compare our method to Wigner function, the most popular tool used to map a wave function onto phase space. The greatest advantage of our method over Wigner function is that our method can smooth out oscillations in wave function without losing any information and produce a probability distribution resembling its classical trajectory. As a result, our

method builds a better quantum-classical connection. In addition, our method has a great potential in signal analysis. In the future, it will be very interesting to generalize our method to quantum spin systems as Wigner function [18].

VIII. ACKNOWLEDGEMENTS

We thank Zhigang Hu for helpful discussion. This work was supported by the The National Key Research and Development Program of China (Grants No. 2017YFA0303302) and the National Natural Science Foundation of China (Grants No. 11334001 and No. 11429402).

-
- [1] R. P. Feynman and A. R. Hibbs, *Quantum Mechanics and Path Integrals* (McGraw-Hill, New York, 1965)
 - [2] E. Wigner, Phys. Rev. **40**, 749 (1932)
 - [3] K. Husimi, Proceedings of the Physico-Mathematical Society of Japan. 3rd Series **22**, 264 (1940)
 - [4] E. C. G. Sudarshan, Phys. Rev. Lett. **10**, 277 (1963)
 - [5] R. J. Glauber, Phys. Rev. **131**, 2766 (1963)
 - [6] *Quantum Mechanics in Phase Space*, edited by C. K. Zachos, D. B. Fairlie, and T. L. Curtright (World Scientific, Singapore, 2005)
 - [7] K. Banaszek, C. Radzewicz, K. Wódkiewicz, and J. S. Krasinski, Phys. Rev. A **60**, 674 (Jul 1999)
 - [8] J. von Neumann, Zeitschrift für Physik **57**, 30 (1929)
 - [9] J. Neumann, The European Physical Journal H **35**, 201 (2010), ISSN 2102-6459
 - [10] X. Han and B. Wu, Phys. Rev. E **91**, 062106 (2015)
 - [11] W. Kohn, Phys. Rev. B **7**, 4388 (May 1973)
 - [12] P. Löwdin, The Journal of Chemical Physics **18**, 365 (1950)
 - [13] J. G. Aiken, J. A. Erdos, and J. A. Goldstein, International Journal of Quantum Chemistry **18**, 1101 (1980)
 - [14] H.-J. Stöckmann, *Quantum Chaos: An Introduction* (Cambridge University Press, Cambridge, 1999)
 - [15] J. Bourgain, Journal of functional analysis **79**, 136 (1988)
 - [16] R. P. Rundle, P. W. Mills, T. Tilma, J. H. Samson, and M. J. Everitt, Phys. Rev. A **96**, 022117 (Aug 2017)
 - [17] L. Cohen, *Time Frequency Analysis* (Prentice Hall, New Jersey, 1994)
 - [18] T. Tilma, M. J. Everitt, J. H. Samson, W. J. Munro, and K. Nemoto, Phys. Rev. Lett. **117**, 180401 (Oct 2016)